ELSEVIER

Thin Solid Films 254 (1995) 175–180

thin solid films

Porosity and composition effects in sol–gel derived interference filters

B. D. Fabes, D. P. Birnie III, B. J. J. Zelinski

Department of Materials Science and Engineering, University of Arizona, Tucson AZ 85721, USA

Received 22 October 1993; accepted 16 June 1994

Abstract

The effects of porosity and composition on the optical thickness of sol–gel films is analyzed using the Clausius–Mossotti relationship. The optical thickness is predicted to decrease with shrinkage approximately linearly. For high density films the predictions agree with experimental data from SiO_2 and $SiO_2-TiO_2-Al_2O_3$ coatings. At low densities, however, the optical thicknesses are much higher than predicted by the Clausius–Mossotti analysis. This difference is attributed to residual species in the unfired films. Using an empirical value for the ratio of the electronic polarizability α_r to the molecular weight W_r of the residual species ($\alpha_r/W_r = 1.65 \times 10^{-25}$ cm^3 mol g^{-1}) the difference between experiment and theory is accounted for quantitatively for both the single-component (SiO_2) and multicomponent ($SiO_2-TiO_2-Al_2O_3$) coatings. Approaches to fabricating multicolor dichroic filters, which require large changes in optical thickness on heating, are presented.

Keywords: Ceramics; Coatings; Ellipsometry; Optical coatings

1. Introduction

Multilayer dichroic filters are stacks consisting of several layers of uniform, transparent films having alternating high and low refractive indices. The films are tailored to be quarter-wave optical thicknesses for the center wavelength for which the filter is designed. A filter results from interference effects which prevent transmission of wavelengths near this center wavelength [1].

For applications requiring large-area filters, stacks can be made by any of a number of vacuum techniques [2] (e.g. evaporation, sputtering, chemical vapor deposition) as well as non-vacuum, sol–gel processes [3–5]. For some imaging or display applications, however, it would be desirable to have selected, small regions that exhibit different colors (e.g. red, green and blue), and for the purpose of miniaturization it would be particularly interesting if these different regions could be closely situated. Photolithographic techniques could be used to deposit small stacks close to one another, but this would require many alignment, masking, and deposition steps. Recently, we suggested an alternative approach, based on the observed change in optical thickness of sol–gel films with heating [6, 7]. After fabricating an entire stack of sol–gel derived high index and low index films (defining one color) small regions were heated using a laser. This transformed the colors of the selected regions, resulting in a patterned dichroic filter. While this demonstrated successfully the concept of selected tuning using laser densification, only a limited range of tunability (about 15%) was achieved. For practical devices it will be necessary to maximize the change in optical thickness that can be achieved in one film; a change of approximately 50%, for example, would be required to produce red, green and blue filters within one stack. The present work is directed towards maximizing the change in refractive index of dielectric films for making three-color dichroic filters.

For sol–gel films both the density and composition can be varied with processing over a wide range, so the potential for producing large changes in optical thickness with processing seems promising. In this paper we examine the effects of these parameters on the change in optical thickness of sol–gel films during processing. First, the effects of porosity and composition are examined analytically, using the Clausius–Mossotti relationship. Next, experimental results from SiO_2 and $SiO_2-TiO_2-Al_2O_3$ films are compared with the predictions, and possible methods for enhancing the change in optical thickness with firing are proposed.

2. Theoretical background

The effects of density and composition on refractive index are given by the Clausius–Mossotti relationship (in CGS units) [8]

$$\frac{\varepsilon^2-1}{\varepsilon^2+1}=\frac{4\pi}{3}\sum_j N_j p_j \tag{1}$$

where ε is the dielectric constant, and N_j is the concentration and p_j the polarizability of species j. At optical frequencies the polarizability arises almost entirely from electronic contributions, so

$$\frac{n^2-1}{n^2+1}=\frac{4\pi}{3}\sum_j N_j\alpha_j \tag{2}$$

where n is the refractive index and α_j is the electronic polarizability. Eq. (2) (the Lorenz–Lorenz equation) can be rearranged by expressing N_j in terms of the molecular weight W_j and weight fraction P_j of species j, density ρ of the material, and Avogadro's number N_A, giving

$$\frac{n^2-1}{n^2+1}=\frac{4\pi\rho N_A}{3}\sum_j \frac{P_j\alpha_j}{W_j} \tag{3}$$

Solving for refractive index gives

$$n=\left(1+\frac{8\pi\rho N_A}{3}\sum_j\frac{P_j\alpha_j}{W_j}\right)^{1/2}\left(1-\frac{4\pi\rho N_A}{3}\sum_j\frac{P_j\alpha_j}{W_j}\right)^{-1/2} \tag{4}$$

so a film of thickness d has optical thickness,

$$nd=(d)\left(1+\frac{8\pi\rho N_A}{3}\sum_j\frac{P_j\alpha_j}{W_j}\right)^{1/2}\left(1-\frac{4\pi\rho N_A}{3}\sum_j\frac{P_j\alpha_j}{W_j}\right)^{-1/2} \tag{5}$$

Experimentally it is usually more convenient to measure the thickness, rather than density, of a film. In terms of thickness the density is $\rho=\rho_0 d_0/d$, where ρ_0 and d_0 are the fully fired, pore-free density and thickness. Thus, if we define the film shrinkage S by

$$S=\frac{d_i-d}{d_i} \tag{6}$$

where d_i is the initial (unfired) film thickness, Eq. (5) can be written

$$nd=[d_i(1-S)]\left(\frac{1+2\beta\sigma}{1-\beta\sigma}\right)^{1/2} \tag{7}$$

where

$$\beta=\frac{4\pi\rho_0 d_0 N_A}{3d} \qquad \sigma=\sum_j\frac{P_j\alpha_j}{W_j} \tag{7a,b}$$

As written, Eq. (7) emphasizes two factors that contribute to optical thickness. The first, $(1-S)$, depends on shrinkage (density) alone; the second, $[(1+2\beta\sigma)/(1-\beta\sigma/)]^{1/2}$, depends on a combination of density (through β) and chemistry (through σ).

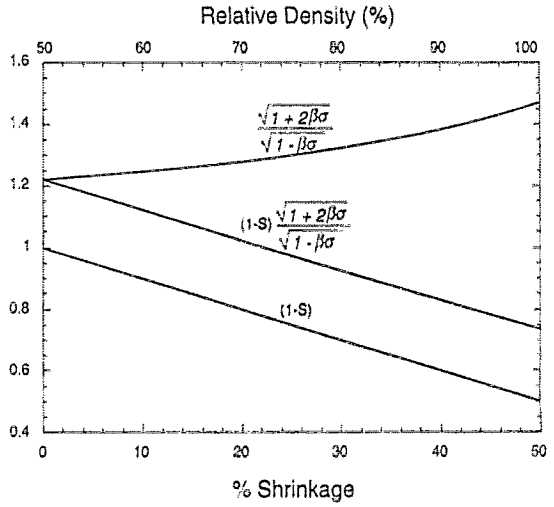

Fig. 1. Shrinkage factor $(1-S)$ and density/chemistry factor $[(1+2\beta\sigma)/(1-\beta\sigma)]^{1/2}$ in predicted optical thickness (Eq. (7)) of typical porous silicate film.

For most conventionally processed, single-component films, the composition should be relatively stable during heating, so we expect that σ = constant. Using typical values for a silicate glass ($\alpha=3\times10^{-24}$ cm^3, $\rho_0=2.2$ g cm^{-3}, $W=60$ g mol^{-1}) the shrinkage and density/composition factors are plotted in Fig. 1 for a film with a total shrinkage of 50%. The shrinkage term $(1-S)$ decreases by 50% (from 1 to 0.5) as the film densifies (shrinks), while the density/chemistry term $[(1+2\beta\sigma)/(1-\beta\sigma)]^{1/2}$ increases by only about 15% (from 1.2 to 1.4) over the same range in shrinkage. Thus, the product $(1-S)[(1+2\beta\sigma)/(1-\beta\sigma)]^{1/2}$, also plotted in Fig. 1, is essentially parallel to the shrinkage term, and the optical thickness, $nd=d_i(1-S)\times[(1+2\beta\sigma)/(1-\beta\sigma)]^{1/2}$ is approximately linear, with a slope of about 1.2–1.4 times the initial film thickness. For relatively dense films, the shrinkage during post-deposition firing should be small, and a correspondingly small change in optical thickness is expected. For relatively porous films, however, large shrinkages should lead to a large decrease in optical thickness.

For multicomponent films and coatings made using sol–gel processing, it is not uncommon for one or more components to volatilize during firing, so that σ is likely to change during processing. This will increase or decrease the net change in optical thickness, depending on the polarizability of the lost components. For example, if high-polarizability species (such as residual organics form sol–gel films) are released, σ will decrease during processing, augmenting the decrease in optical thickness caused by densification and the overall change in nd will be increased. The release of low index components, however, would increase σ progressively, offsetting the decrease in optical thickness due to densification, and the overall change in nd would be lessened.

3. Experimental procedures

To examine experimentally the effects of density and composition on the change in refractive index of porous coatings, both single-component (SiO_2) and multicomponent ($SiO_2-TiO_2-Al_2O_3$) films were examined.

3.1. Coating preparation

For sol–gel derived coatings SiO_2 solutions were made by mixing 4 mol ethanol with 1 mol tetraethoxysilane (TEOS) and then hydrolyzing the solution by adding 2 mol of acidified water (0.36 M HCl) to bring the final solution pH to 2 [9]. Coatings were formed by dipping double-polished silicon substrates into the solution in air (20–22 °C, 25%–35% relative humidity) and withdrawing at a constant rate. Immediately after coating all samples were dried in air at 100 °C, resulting in 200–250 nm thick porous coatings. Samples were fired, in air, by placing the dried coatings directly into a hot furnace for 15 min.

Following the work of Weisenbach [10], $SiO_2-TiO_2-Al_2O_3$ coating solutions with a target composition of approximately $2SiO_2 \cdot 2TiO_2 \cdot Al_2O_3$ were prepared by diluting 0.42 mol TEOS with 0.042 mol dried ethanol at 60 °C. To this solution 0.042 mol of 0.15 M HCl was added dropwise, and the solution was then stirred for 30 min. In a separate flask 0.044 mol Ti(IV) ethoxide was mixed with 0.042 mol Al sec-butoxide, and allowed to mix for 15 min, after which 1.25 mol dry ethanol was added. Small white precipitates were formed initially, but then redissolved. After 15 min the TEOS solution was slowly poured into the Ti–Al solution, and the combined solution was allowed to mix under ambient conditions (22 °C, 34% RH) for at least 12 h.

Coatings were formed by diluting this solution with ethanol to 10 wt.% solids, filtering through 0.2 μm filters, and spinning onto polished Si wafers at 2250 rev min^{-1} for 24 s. After coating each film was placed immediately in the center of a pre-heated furnace and fired for 15 min at the temperature of choice.

3.2. Analysis

Multiple angle ellipsometry was used to determine refractive index and sample thickness. Measurements were taken at 60°, 65°, and 70°, and the thickness and refractive index were calculated assuming $k_{Si} = 0.02$, $n_{Si} = 3.871$, and $k_{film} = 0.0$.

The composition of the multicomponent glass films was determined experimentally by Rutherford backscattering (RBS) using a 3.8 MeV He^{2+} beam and a total charge of 120 μC.

4. Results

The changes in optical thickness with firing for both single-component and multicomponent coatings are shown in Fig. 2. As expected, the optical thickness decreases as the firing temperature increases, up to approximately 1000 °C for the sol–gel derived SiO_2 film, and 800 °C for the $SiO_2-TiO_2-Al_2O_3$ coating. At higher temperatures the thickness, index, and hence optical thickness, are essentially constant, indicating that the films are fully dense.

The starting and fired compositions of the $SiO_2-TiO_2-Al_2O_3$ samples are shown in Table 1. The composition of the film is close to the target composition, and remains essentially unchanged during firing.

5. Discussion

To facilitate comparison between films, the changes in optical thickness are plotted against shrinkage in Figs. 3(a) and (b). The solid lines are the theoretical change in optical thickness, as predicted by the Clausius–Mossotti analysis, assuming constant composition. For the SiO_2 films this line was calculated by first determining an effective polarizability of the SiO_2 glass ($\alpha_{SiO_2} = 2.92 \times 10^{-24}$ cm^3) using Eq. (3) and theoretical values of the refractive index ($n_{SiO_2} = 1.45$) and density ($\rho_0 = 2.2$ g cm^{-3}) of SiO_2. The theoretical predictions

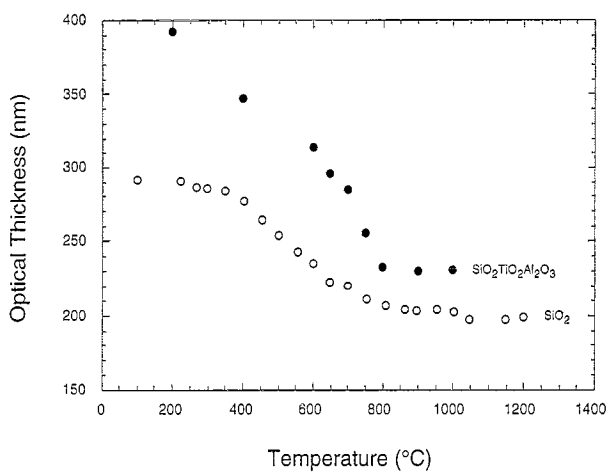

Fig. 2. Optical thickness of sol–gel derived SiO_2 and $SiO_2-TiO_2-Al_2O_3$ films vs. firing temperature.

Table 1
Compositional analysis of $SiO_2-TiO_2-Al_2O_3$ films in weight per cent

	Solution	500 °C	700 °C
SiO_2	30.8	29.4 ± 2.2	30.4 ± 2.1
TiO_2	43.0	43.8 ± 2.3	41.6 ± 1.7
Al_2O_3	26.2	26.8 ± 1.9	28.0 ± 1.7

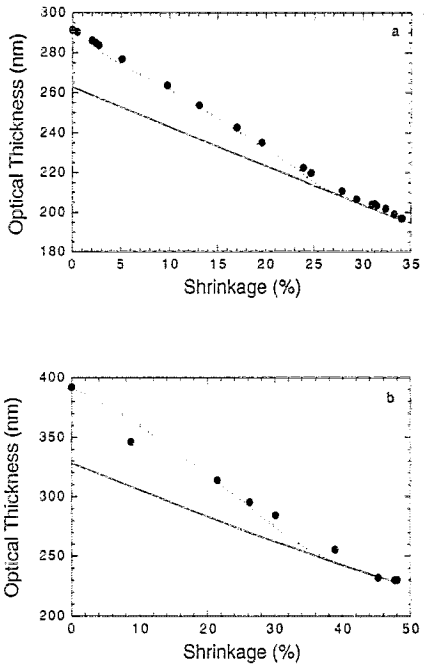

Fig. 3. Optical thickness of (a) sol–gel derived SiO_2 films, and (b) sol–gel derived SiO_2–TiO_2–Al_2O_3 films vs. firing temperature. Filled circles are experimental data, solid lines are theoretical calculations using Eq. (7), without accounting for residual species, and dashed lines are theoretical calculations using Eq. (7), with allowance made for residual species.

were then derived using Eq. (7). For multicomponent films the theoretical predictions were calculated, as for SiO_2, using an effective polarizability of the glass ($\alpha_g = 3.98 \times 10^{-24}$ cm^3) which was determined, in turn, using Eq. (3) and theoretical values of density and refractive index. For the SiO_2–TiO_2–Al_2O_3 films the theoretical density was calculated by the weighted average of the densities of the constituents, giving $\rho_0 = 3.40$ g cm^{-3}, and the theoretical refractive index was calculated using the method of Huggins and Sun [11] giving $n_g = 1.85$.

5.1. Single-component films

At high shrinkage (density) the measured optical thickness of the SiO_2 films agrees with that predicted by Eq. (7) and, as expected, the optical thickness decreases roughly linearly with shrinkage. For lower density films, however, the change in optical thickness is non-linear, with experimental values exceeding the predicted values more radically at lower density. This departure from linearity is most probably the result of residual species in the sol–gel film, which increase the effective index and, hence, optical thickness of the lower density films.

Accounting quantitatively for the contribution of residual species would require a knowledge of the concentration P_r, molecular weight W_r, and polarizability α_r of each of the n residual species,

$$\sigma = \sum_j \frac{P_j \alpha_j}{W_j} = \frac{P_{SiO_2}\alpha_{SiO_2}}{W_{SiO_2}} + \frac{P_{r_1}\alpha_{r_1}}{W_{r_1}} + \frac{P_{r_2}\alpha_{r_2}}{W_{r_2}} + \cdots + \frac{P_{r_n}\alpha_{r_n}}{W_{r_n}} \quad (7b)$$

Weisenbach [10] recently analyzed the effects of residual water on the polarizability (and hence refractive index) of sol–gel derived silica–titania films using Eq. (7b). By heating films to temperatures where organics were removed, the effects of residual organics could be ignored. By approximating the effect of dissolved water on the connectivity of the oxide network, Weisenbach proposed a structure for the films and then, by assigning different polarizabilities to adsorbed water, to water dissolved in the structure, to bridging oxygen atoms, and to non-bridging oxygen atoms, she was able to account quantitatively for the changes in refractive index with heating.

While the success of Weisenbach's approach lends validity to the present approach for analyzing these films, the effects of residual organics, in addition to water, would need to be taken into account to develop a structural model for the present films. Lacking such a model, we simplify the analysis by grouping the residual species (organics and water) into one term, and we define the ratio of polarizability to molecular weight as a constant R which gives

$$\sigma = \sum_j \frac{P_j \alpha_j}{W_j} = R_{SiO_2} P_{SiO_2} + R_r P_r \quad (8)$$

where $R_{SiO_2} = \alpha_{SiO_2}/W_{SiO_2}$ and $R_r = \alpha_r/W_r$, the subscript r referring to the residual species.

Eq. (8) can be solved for an empirical value of R_r using experimental thermogravimetric analysis data [12] to approximate the total concentration of residual species in the unfired gel ($P_r = 18$ wt.%) the measured optical thickness of the unfired gel ($nd = 291$ nm at 100 °C) and by noting that $P_{SiO_2} + P_r = 1$. The resulting empirical value, $R_r = 1.65 \times 10^{-25}$ cm^3 mol g^{-1}, is within a factor of two of the R_r of other species (e.g. $R_{ethanol} = 1.15 \times 10^{-25}$ cm^3 mol g^{-1}, $R_{water} = 8.09 \times 10^{-26}$ cm^3 mol g^{-1}) that are likely to compose a large portion of the residue in sol–gel films.

Assuming that R_r is constant during firing, and that the concentration of residual species decreases parabolically [12, 13] from the experimental value (18 wt.%) at 100 °C to 0 wt.% at 750 °C, the predicted change in optical thickness is plotted as the dashed line in Fig. 3(a). Using this method the calculated and measured values of optical thickness are by definition equal for the unfired film. Theory and experiment agree well over the entire range of shrinkages, indicating that R_r changes only slightly during firing. Using a constant value of R_r therefore allows us to separate conveniently the contributions to optical index from shrinkage and

chemistry, without having to hypothesize a detailed model of the composition and microstructure of the film.

5.2. Multicomponent film

As with SiO_2 films, the optical thickness of sol–gel derived $SiO_2-TiO_2-Al_2O_3$ films decreases with shrinkage (Fig. 3(b)). At high densities the change in optical thickness with shrinkage is linear and the predicted values agree with those measured, and at low densities the change in optical thickness is greater than predicted. Assuming that the discrepancy at low densities is caused again by residual species, the expected change in optical thickness can be calculated using the empirical value $R_r = 1.65 \times 10^{-25}$ cm^3 mol g^{-1} (assuming that the composition of the residual species is similar to that in the SiO_2 films). Lacking experimental data for P_r for this system, we can use Eq. (5) and the measured optical thickness for the porous (200 °C) film to solve for the initial concentration of residuals, giving $P_r = 26$ wt.% at 200 °C. Finally, assuming, again, that R_r is constant during firing, and that the concentration of residuals decreases parabolically from a concentration of 26 wt.% at 200 °C to 0 wt.% at 750 °C, the predicted change in optical thickness is plotted as the dashed line in Fig. 3(b). Again, the nature of the calculation forces agreement between experiment and theory for the dried (200 °C) film, but agreement is relatively good over the entire range of shrinkage, especially considering the approximate nature of the change in residual content with temperature and the likelihood that the composition of the residual species changes during firing.

5.3. Application to color filters

For applications where a large change in optical thickness with firing is desired, the higher porosity of as-deposited sol–gel films, and resulting larger range of densities over which such films can be varied, makes sol–gel derived films preferable to films formed by evaporation, or other methods which result in coatings with relatively high densities. Moreover, the volatilization of residual species can enhance the change in optical thickness during firing of the sol–gel films. In this study, for example, the optical thickness of the $SiO_2-TiO_2-Al_2O_3$ films decreased more than 40%, without any special attention paid to optimizing the change. Still, larger changes in optical thicknesses (at least 50%) will be required to produce practical devices, so films which shrink even more than xerogel films (e.g. aerogel coatings) might be required. It will be important to evaluate the mechanical and chemical stability of extremely porous films though, as they might not have the robustness needed for practical devices.

Another approach to fabricating stable, tunable filters might be to use a multicomponent film from which a high index species is volatilized during firing. As discussed previously, this would decrease σ during firing, thereby enhancing the change in optical thickness with densification. Future investigations should explore this possibility, paying attention to the stability of the volatile component in the unfired or partially-fired materials.

The Clausius–Mossotti analysis suggests also that the rate of heating might affect the change in optical thickness, especially for multicomponent films. If highly polarizable species (e.g., organics, or PbO in multicomponent films) are lost during processing, faster heating, such as with a laser, is likely to minimize volatilization and the change in *nd* during processing will arise solely from shrinkage. In such cases the largest decrease in optical thickness would be expected to occur with slow heating, which would maximize volatilization. Conversely, rapid heating is expected to increase the change in *nd* during processing of films which lose low polarizability species during processing, since fewer volatiles would be lost. These possibilities remain unexplored.

6. Summary

For high density films in which composition is constant, the Clausius–Mossotti analysis predicts that optical thickness should vary approximately linearly with shrinkage. This is found experimentally for single-component and multicomponent sol–gel films, although the loss of residual species during firing must be taken into account to predict the change in optical thickness over a wide range of densities. Using an empirical value, $R_r = \alpha_r / W_r = 1.65 \times 10^{-25}$ cm^3 mol g^{-1}, the change in optical thickness of sol–gel films can be predicted over a wide range of temperatures (densities). For applications where large changes in optical thickness with density are desired, sol–gel films are advantageous owing to their high porosity. Changes in *nd* of over 40%, for example, were achieved in this study. To maximize the change in *nd* in practical systems, extremely porous films, and compositions with volatile high index components are suggested, although the stability at low firing temperatures must be examined.

Acknowledgements

The experimental data analyzed in this study were provided by Greg Lostracco and Doug Taylor. Their input, and the guiding suggestions of Sharon Melpolder, are gratefully acknowledged. Financial support has been provided generously by the Donnelly Corporation.

References

[1] H. A. Macleod, *Thin-Film Optical Filters*, Hilger, Bristol, 1986, 2nd edn.

[2] R. W. Phillips and J. W. Dodds, Optical interference coatings prepared from solution, *Appl. Opt.*, *20* (1) (1981) 40–47.

[3] D. P. Partlow and T. W. O'Keeffe, Thirty-seven layer optical filter from polymerized sol–gel solutions, *Appl. Opt.*, *29* (1990) 1526–1529.

[4] J. L. Keddie and E. P. Giannelis, Optical interference filters by sol–gel processing, *Mater. Res. Soc. Symp. Proc.*, *180* (1988) 387–392.

[5] S. M. melpolder, M. J. Hanrahan and G. N. Musshafen, Preparation of intereference filters using low-temperature sol–gel processing. In L. L. Hench and J. K. West (eds.), *Chemical Processing of Advanced Materials*, Wiley, New York, 1992, pp. 437–447.

[6] D. P. Birnie III, S. M. Melpolder, B. D. Fabes, B. J. J. Zelinski and M. J. Hanrahan, Laser processing of sol–gel derived multilayer interference filters, *Sol–Gel Optics II: SPIE Proc.*, *1758* (1992) 630–637.

[7] D. P. Birnie III, S. M. Melpolder, B. D. Fabes, B. J. J. Zelinski and M. J. Hanrahan, Laser processing of chemically derived dichroic filters, *Opt. Eng.*, *32* (1993) 2960–2965.

[8] C. Kittel, *Introduction to Solid State Physics*, Wiley, New York, 1976.

[9] D. J. Taylor and B. D. Fabes, Laser processing of sol–gel coatings, *J. Non-Cryst. Solids*, *147–148* (1992) 457–462.

[10] L. Weisenbach, Processing characteristics and optical properties of wet-chemically derived planar dielectric waveguides, *PhD Dissertation*, University of Arizona, Tucson, AZ, 1993.

[11] M. L. Huggins and K. Sun, Calculation of density and optical constants of a glass from its composition in weight percentage, *J. Am. Ceram. Soc.*, *26* (1) (1943) 4–11.

[12] M. Yamane, S. Aso, S. Okano and T. Sakaino, Low temperature synthesis of a monolithic silica glass by the pyrolysis of a silica gel, *J. Mater. Sci.*, *14* (1979) 607–611.

[13] G. Carturan, V. Gottardi and M. Graziani, Physical and chemical evolutions occurring in glass formation from alkoxides of silicon, aluminum and sodium, *J. Non-Cryst. Solids*, *29* (1978) 41–48.